GPS Solut (2017) 21:1191–1201
DOI 10.1007/s10291-017-0602-0

ORIGINAL ARTICLE

Improving BDS integer ambiguity resolution using satellite-induced code bias correction for precise orbit determination

Tao Geng[1,2] · Xin Xie[1] · Qile Zhao[1,2] · Xianglin Liu[3] · Jingnan Liu[1,2]

Received: 4 September 2016 / Accepted: 23 January 2017 / Published online: 4 February 2017

Abstract Successful resolution of integer ambiguity over long baselines is a key to improve the accuracy of precise orbit determination for global navigation satellite system satellites. The satellite-induced code bias (SCB) found in BDS signals severely prevents the BDS integer ambiguity resolution (AR) of long baselines. We present BDS AR using satellite-induced code bias correction for precise orbit determination. The impacts of the BDS SCB on double-difference AR for different baseline length and satellite type are first assessed. About one month of BDS tracking data collected from the MGEX and Fugro network are processed for precise orbit determination using independent single-system method. The results of orbit overlap comparison and satellite laser ranging (SLR) validation suggest that the SCB has no obvious impacts on BDS float solutions; however, it shows significant implications on ambiguity-fixed solutions, especially for MEO satellites and long baselines. When applying the SCB correction model to BDS AR, the 3D mean RMS of overlapping orbit are reduced from 14.02 to 10.46 cm for IGSO and from 10.97 to 6.89 cm for MEO satellite, with the improvement of 25.4 and 37.2%. The contribution of AR with SCB correction on orbit accuracy of BDS could reach the level close to that of GPS. SLR residuals also confirm the improvement.

Keywords GNSS · Integer ambiguity resolution · Precise orbit determination · Satellite-induced code bias · Code pseudorange

✉ Tao Geng
gt_gengtao@whu.edu.cn

✉ Qile Zhao
zhaoql@whu.edu.cn

[1] GNSS Research Center, Wuhan University, 129 Luoyu Road, Wuhan 430079, China

[2] Collaborative Innovation Center of Geospatial Technology, 129 Luoyu Road, Wuhan 430079, China

[3] Fugro Intersite B.V., 2263 HW Leidschendam, The Netherlands

Introduction

The BeiDou Navigation Satellite System (BDS) was officially declared to be operational as a regional system, i.e., phase two, on December 27, 2012 (CSNO 2013). The constellation in this phase consists of 14 satellites, five geostationary orbit (GEO), five inclined geostationary orbit (IGSO), and four medium earth orbit (MEO), transmitting triple-frequency signals centered at B1 (1561.098 MHz), B2 (1207.14 MHz), and B3 (1268.52 MHz). However, satellite C13 of these 14 satellites is currently unavailable.

Precise orbit determination (POD) is of great significance for enhancing GNSS positioning, navigation and timing (PNT) service. In recent years, BDS POD and GPS/BDS combined POD have been investigated (Montenbruck et al. 2012; Shi et al. 2012; Zhao et al. 2013; Guo et al. 2015; Li et al. 2015). With the establishment of the multi-GNSS experiment (MGEX, Montenbruck et al. 2014) by the International GNSS Service (IGS, Dow et al. 2009), several analysis centers (ACs) have provided BDS precise orbit and clock products since 2013, e.g., the Center for Orbit Determination in Europe, GeoForschungsZentrum, the European Space Agency, and Wuhan University. The quality assessment for BDS orbit products provided by MGEX ACs shows the 3D accuracy is at decimeter to meter level for GEO, 0.2–0.3 m for IGSO, and 0.1-0.2 m for MEO satellites (Guo et al. 2015, 2016a). Also, some

aspects affecting the orbit quality of BDS POD have also been investigated. Steigenberger et al. (2013) and Lou et al. (2014) tested the BDS POD solutions for different data arc lengths and solar radiation pressure (SRP) parameters. He et al. (2013) and Zhang et al. (2015) analyzed the impact of tracking station distribution on BDS POD. Dai et al. (2015) investigated attitude control mechanism of BDS IGSO and MEO satellites and their effect on orbits. The orbit products of BDS IGSO and MEO satellites determined by different SRP models were compared by Guo et al. (2016b).

Despite these efforts, the accuracy of the radial component of BDS IGSO and MEO orbits is still markedly worse than that of GPS. One of the major reasons is that the GPS POD solutions significantly improves by successful ambiguity resolution (AR) even over baselines up to several thousand kilometers (Blewitt 1989; Ge et al. 2005). For BDS, recent researches on AR were mainly focusing on short baselines or regional networks (Shi et al. 2013; Qu et al. 2015). The combination with GPS data (Gao et al. 2015; Liu et al. 2016) and using three-frequency (Zhang and He 2015; Zhao et al. 2015) were considered. There is not much discussion on BDS AR for long baselines, which is often the case in POD. Until now, none of the MGEX ACs has reported AR for their routine data processing of BDS POD.

Although He et al. (2013) carried out BDS AR in POD, and assessed the impact of AR on orbit products, the orbit overlap comparison exhibited that the radial accuracy was not improved. The 3D RMS improved by 30% for IGSO and only 6% for MEO satellites, respectively, which is not comparable with that of GPS AR. There is still room for improvement on BDS orbit quality by AR. The signal quality is one of the most important factors affecting GNSS AR. Some studies have revealed that there is a different characteristic for BDS code signals compared with other GNSS ones (Hauschild et al. 2012; Gisbert et al. 2012; Montenbruck et al. 2013; Wanninger and Beer 2015), namely the satellite-induced code bias (SCB). This SCB can vary more than 1 m from horizon to zenith, which would affect BDS code measurement model and wide-lane AR based on the Hatch–Melbourne–Wübbena (HMW) combination (Hatch 1982; Melbourne 1985; Wübbena 1985). The SCB is not relevant to the type of GNSS receiver and is likely attributed to the internal satellite multipath, which is elevation dependent. Therefore, the elevation-dependent correction model was proposed by Wanninger and Beer (2015) for IGSO and MEO satellites for each of the three frequencies (B1, B2, and B3). Subsequently, Lou et al. (2016) modeled the SCB for GEO satellites based on the single-differenced fractional cycle bias and assessed the effects of the SCB on AR. For double-difference (DD) AR, the effects of the SCB could be weakened or eliminated on short baseline or zero baseline because both station see the same satellite at approximately the same elevation, but might amplify on long baseline due to different elevations. Since the tracking network used in POD consists mainly of long baselines, it is meaningful to investigate BDS AR with SCB correction for POD to improve the orbit quality further.

We give a theoretical analysis why the SCB correction model is required for the BDS long baseline AR. We assess the impacts of the BDS SCB on DD AR for different baseline length and satellite type by comparing the results without and with SCB corrections. Furthermore, the BDS POD results from four different solutions, i.e., float solutions, float solutions with SCB correction, AR solutions, and AR solutions with SCB correction are evaluated by orbit overlap differences and SLR validation.

Methodology

Since there are significant elevation-dependent and frequency-dependent systematic biases in BDS code observations, which would affect directly the pseudorange observation model and the HMW linear combination, we introduce the observation equations with the SCB correction model involved in BDS POD AR.

Basic observation models

Considering the effects of the SCB, the BDS undifferenced observation equations for the dual-frequency carrier phase and pseudorange from receiver r to satellite s, in units of length, are

$$\begin{aligned} L^s_{r,f} &= \rho^s_r - I^s_{r,f} + \lambda_f B^s_{r,f} \\ P^s_{r,f} &= \rho^s_r + I^s_{r,f} - d^s_f(E) \end{aligned} \tag{1}$$

where $L^s_{r,f}$ and $P^s_{r,f}$ are, respectively, the carrier phase and pseudorange measurements on frequency f ($f = 1, 2$) with corresponding wavelength λ_f, and ρ^s_r is the non-dispersive delay, including geometric distance, tropospheric delay, satellite and receiver clock biases, satellite orbit errors, and any other delay which affects all the observations identically. $I^s_{r,f}$ is the ionospheric delay, $B^s_{r,f}$ is the non-integer phase ambiguity, i.e., $B^s_{r,f} = N^s_{r,f} + \delta\phi_{r,f} - \delta\phi^s_f$, where $N^s_{r,f}$ is the zero-difference (ZD) integer ambiguity, $\delta\phi_{r,f}$ and $\delta\phi^s_f$ are uncalibrated phase delays (UPDs) in receiver and satellite transmitter, respectively. Further, $d^s_f(E)$ is the SCB error modeled as a function of elevation, with E representing the elevation angle. The multipath error and noise are ignored for brevity.

The ionospheric-free observation is used in POD data processing to remove the first-order effect of ionospheric delay (Kouba and Héroux 2001),

$$L^s_{r,c} = \frac{f_1^2}{f_1^2 - f_2^2} L^s_{r,1} - \frac{f_2^2}{f_1^2 - f_2^2} L^s_{r,2} = \rho^s_r + \lambda_1 B^s_{r,c}$$
$$P^s_{r,c} = \frac{f_1^2}{f_1^2 - f_2^2} P^s_{r,1} - \frac{f_2^2}{f_1^2 - f_2^2} P^s_{r,2} = \rho^s_r + \frac{f_2^2 \cdot d^s_2(E) - f_1^2 \cdot d^s_1(E)}{f_1^2 - f_2^2} \quad (2)$$

where $B^s_{r,c}$ denotes the float ionospheric-free ambiguity.

Ambiguity resolution

For AR, the float ionospheric-free ambiguity is usually expressed as the combination of wide-lane (WL) ambiguity and narrow-lane (NL) ambiguity,

$$B^s_{r,c} = \frac{f_1 f_2}{f_1^2 - f_2^2} B^s_{r,w} + \frac{f_1}{f_1 + f_2} B^s_{r,n} \quad (3)$$

where $B^s_{r,c}$ is the ionospheric-free ambiguity, $B^s_{r,w}$ and $B^s_{r,n}$ are WL and NL ambiguities.

The WL ambiguity can be derived with the HMW combination of the carrier phase and code observations. The BDS HMW combination from receiver r to satellite s in cycle can be expressed as:

$$L^s_{r,w} = \left(\frac{L^s_{r,1}}{\lambda_1} - \frac{L^s_{r,2}}{\lambda_2}\right) - \left(\frac{f_1 P^s_{r,1} + f_2 P^s_{r,2}}{(f_1 + f_2)\lambda_w}\right) = B^s_{r,w} + D^s_w(E) \quad (4)$$

with

$$D^s_w(E) = \frac{f_1 \cdot d^s_1(E) + f_2 \cdot d^s_2(E)}{(f_1 + f_2)\lambda_w} \quad (5)$$

$$B^s_{r,w} = N^s_{r,w} + \delta\phi_{r,w} - \delta\phi^s_w \quad (6)$$

where $L^s_{r,w}$ is the HMW combination, λ_w is the WL wavelength, $D^s_w(E)$ represents the effect of SCB on WL, $N^s_{r,w}$ is the WL integer ambiguity, and $\delta\phi_{r,w}$ and $\delta\phi^s_w$ are UPDs for receiver and satellite which can be eliminated by the DD between two satellites and two receivers.

From (4) and (5), the DD WL ambiguity between two satellites $(s1, s2)$ and two receivers $(r1, r2)$ becomes:

$$\Delta\nabla B_w = \Delta\nabla L_w - \Delta\nabla \mathrm{D}_w \quad (7)$$

with

$$\Delta\nabla \mathrm{D}_w = \left(D^{s1}_w(E^{s1}_{r1}) - D^{s1}_w(E^{s1}_{r2})\right) - \left(D^{s2}_w(E^{s2}_{r1}) - D^{s2}_w(E^{s2}_{r2})\right) \quad (8)$$

where $\Delta\nabla$ represents the DD operation, $\Delta\nabla L_w$ is the DD HMW combination, $\Delta\nabla B_w$ is the DD WL ambiguity having integer feature, $\Delta\nabla \mathrm{D}_w$ is the DD WL SCB, and E^s_r represents the elevation angle from satellite s to receiver r.

From (7) and (8), the UPDs of receiver and satellite are eliminated when applying the DD operation. However, this is not the case for the SCB error. The effects of SCB on the DD WL are eliminated or reduced for short baselines due to viewing the satellites at approximately the same elevation. However, it might be amplified, or at least not be sufficiently reduced, on baselines longer than a few hundred kilometers, as their elevations are very different. In that case, the effects may remain in the float ambiguity terms as a bias and spoil the integer nature of DD WL ambiguities. Therefore, it is necessary to remove them using a proper modeling. We use the elevation-dependent correction models presented by Wanninger and Beer (2015). The SCB correction values $d^s_f(E)$ are obtained by linear interpolation of model parameters according to elevation angle and inserted into the pseudorange observation Eq. (1).

We follow the procedure of ambiguity fixing in Ge et al. (2005), i.e., first fixing the geometry-free WL ambiguity integers and then fixing geometry-based NL float ambiguities. To do so, the average of DD ambiguities over the epochs in a pass and its variance are calculated. With the ambiguity estimates and their variances, the fixing decision can be made according to the probability function proposed by (Dong and Bock 1989) as follows,

$$P = 1 - \sum_{i=1}^{\infty} \left[\mathrm{erfc}\left(\frac{i - |b - n|}{\sqrt{2}\sigma}\right) - \mathrm{erfc}\left(\frac{i + |b - n|}{\sqrt{2}\sigma}\right)\right] \quad (9)$$

where b and σ are the estimate and its variance, respectively, and n is the nearest integer candidate for the estimate b. Taking the confidence level α as 0.1%, the ambiguity can be fixed to the nearest integer if the fixing probability P is larger than $1 - \alpha$; otherwise, it should remain unfixed.

Only after successfully fixing the WL can the NL ambiguity be resolved based on the fixed WL and the estimated float ionospheric-free ambiguity,

$$\Delta\nabla B_n = \frac{f_1 + f_2}{f_1} \Delta\nabla B_c - \frac{f_2}{f_1 + f_2} \Delta\nabla N_w \quad (10)$$

where N_w is the fixed integer value of the WL ambiguity and B_c is the estimate of ionospheric-free ambiguity calculated based on the real-valued solution. Similarly, to the WL ambiguity, we get the fixing probability for the NL ambiguity from its estimate and variance and then make the fixing decision. We mention that the NL ambiguities are mainly determined from carrier phase measurements, because the relative weighting of carrier phase and pseudorange is usually larger than 10,000:1. The SCB error has no significant effect on NL AR (Lou et al. 2016). We will not pay attention on this respect.

Once both WL and NL ambiguities are fixed, these integer ambiguities are used to reconstruct the ionospheric-free ambiguities according to (3). The DD ambiguities are

Table 1 Receiver type distribution from MGEX and Furgro network used in this study

Receiver type	MGEX	Fugro
Trimble NETR9	19	26
Septentrio PolaRx4	7	0
Septentrio PolaRx4TR	2	0
Leica GR10	3	0
Leica GR25	1	0

mapped back to the undifferenced ambiguities, and their corresponding constraints are imposed to the normal equation system for computing other parameters, resulting in the so-called the ambiguity-fixed solution.

Data collection

In order to validate the impact of BDS AR with SCB correction on POD, we process BDS tracking data of 58 GNSS stations from February 1 (DOY 032) to March 2 (DOY 063), 2015. Thirty-two stations are equipped with different types of receiver from the MGEX network (Montenbruck et al. 2014). The other 26 stations are from a worldwide reference station network operated by Fugro for supporting its commercial positioning services, mainly for maritime applications (Tegedor et al. 2014). Table 1 summarizes the receiver types of selected stations. Figure 1 shows the geographic distribution of these GNSS stations. We note that there is no dependence of the BDS SCB on receiver types according to (Wanninger and Beer 2015).

Processing strategy

The positioning and navigation data analyst (PANDA) software package (Liu and Ge 2003; Shi et al. 2008), developed at GNSS Research Center of Wuhan University (WHU), is adapted for BDS POD. There are two different methods of data processing: (1) All parameters are estimated only from BDS observations without using other GNSS observations. (2) Simultaneous observations from other GNSS or their derived common parameters, such as station coordinates, receiver clocks, and zenith tropospheric delay, are involved in BDS POD. The former method, which can demonstrate the performance of BDS as a fully independent navigation system, is adopted in this contribution.

We take three consecutive days as one orbit arc and process BDS data of these days to obtain a three-day solution in a batch mode. For each three-day solution, the ionospheric-free linear combinations of B1 and B2 are used to form basic observation equations to eliminate the ionospheric delay. The prior orbits are taken from the broadcast

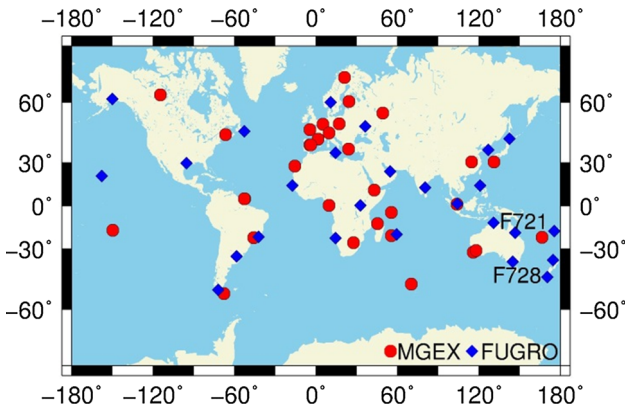

Fig. 1 Distribution of selected MGEX (*red circle*) and Fugro (*blue diamond*) stations used in this study

ephemeris provided by the MGEX. The BDS satellite orbit parameters, which include initial position and velocity and SRP parameters, and the satellite clock offsets, station coordinates, receiver clock biases, float ambiguities, and 2-h zenith total delay (ZTD) parameters are estimated. For BDS IGSO and MEO satellites, the antenna phase center offset (PCO) and phase center variation (PCV) corrections provided by WHU are used because of their improved performance (Guo et al. 2015). Table 2 lists the observation models, dynamical models, and estimated parameters applied in BDS POD processing.

The integer ambiguities are resolved using the approach described above. Baseline length is limited to 3500 km. For each selected independent baseline, any DD ambiguity with observation segment longer than 20 min is considered. Otherwise, these observations are discarded. We point out that the ambiguities of BDS GEO satellites (C01-C05) are not fixed in this study because of their weak tracking geometry. The weak geometry strength results in larger orbit biases in the along-track direction, which may be up to several meters. Ge et al. (2012) found that the along-track orbit biases of GEO are highly correlated with the ambiguity parameters and difficult to separate even with three days of data. He et al. (2013) indicated that the satellite orbits become worse after fixing ambiguities of GEO, which is likely a result of incorrectly fixing ambiguities. Therefore, we only discuss the IGSO and MEO satellites AR performance and compare their orbit qualities in the next section, though the GEO satellites are also included in POD processing.

Influence of SCB on WL AR

Figure 2 shows the time series of DD WL ambiguities for three types of satellite pairs (IGSO–IGSO, IGSO-MEO, MEO–MEO) with and without SCB correction as examples. The elevation differences of each satellite tracked by

Table 2 Observation models, dynamical models, and estimated parameters for BDS POD

Item	Models
Observables	Undifferenced ionospheric-free code and phase combination of B1 and B2
Sampling rate	30 s
Arc length	3 days
Elevation cutoff	10°
Weighting	Priori precision of 0.002 m and 2.0 m for raw phase and code observables, respectively, and elevation-dependent data weighting
Satellite antenna phase center	PCO and PCV corrections using WHU estimated values
Receiver antenna phase center	Corrections for GPS L1 and L2 are used for BDS B1 and B2, igs08.atx
Phase wind up	Phase polarization effects applied
Ionospheric delay	First-order effect eliminated by forming the ionospheric-free combination of B1 and B2
Tropospheric delay	Saastamoinen model for wet and dry hydrostatic delay with GMF mapping function, estimated as piecewise constant function with 2-h parameter spacing for residual wet delay
Station coordinates	Estimated
Receiver clocks	Estimated as random walk process for each epoch
Satellite clocks	Estimated as random walk process for each epoch
Satellite orbit	Estimated
Phase ambiguities	Real constant for each ambiguity arc; DD AR for network solution
EOP parameters	IERS C04 Fixed
Tide displacement	Solid Earth tide, pole tide, ocean tide loading; IERS Convention 2003 (McCarthy and Petit 2003)
Relativity effect	IERS Conventions 2003
Geopotential	EIGEN_GL04C up to 12 × 12
N-body gravitation	Sun, Moon, and other planets; JPL DE405 ephemeris used
Solar radiation	ECOM model 5-parameter with no initial value (Springer et al. 1999)
Attitude model	Nominal attitude with yaw maneuver for MEO and IGSO satellites; the yaw-fixed attitude mode used for GEO satellites

two stations separated by about 2000 km are also plotted. As can see, the effects of the SCB on WL could not be eliminated by DD for long baseline due to different elevations of two stations. Also, the SCB exerts larger impacts on MEO, which is due to the faster-changing elevation of MEO having the lower orbit as shown in the middle part of the figure. After application of the correction models, these biases are removed or largely reduced for all satellite pairs as shown in the bottom panels, which proves the success of the SCB correction model.

For all GNSS stations used in our POD, the number of independent baselines shorter than 3500 km for every arc is almost the same, which about 53. Taking the arc of DOY 036 - 038 as an example, the distribution of baseline length is shown in Fig. 3. To assess the effects of SCB on all independent baselines in Fig. 3 for IGSO and MEO satellites, we plot the distribution histogram of the fractional parts of all DD WL ambiguities for different satellite pairs during the experiment period, as shown in Fig. 4. The quantized nature of these fractional values and the characteristic Gaussian shape of the distribution can be seen, which confirms the reasonability of our results. It is clear that the application of the SCB correction reduces the average RMS of fractional parts significantly from 0.180, 0.226, and 0.247 cycles (top panels) to 0.161, 0.165, and 0.176 cycles (bottom panels) for IGSO–IGSO, IGSO-MEO, and MEO–MEO pairs. This is an improvement of 10.6%, 27.0%, and 28.7%, respectively. From (9), under rounding criteria, such an improvement significantly increases the success rates of DD WL ambiguity fixing.

We group the baselines by length of 500 km to analyze the impacts of the BDS SCB on WL AR for different baseline length. The percentages that fractional cycles of all independent DD WL ambiguities in a group fall within ± 0.2 cycles are shown in Fig. 5. For those MEO–MEO satellite pairs, the SCB correction significantly increases the percentages, particularly for baselines longer than 1000 km. This improvement will increase the success rates of DD WL ambiguity fixing, providing more possibility for DD NL ambiguities to be fixed. For IGSO-MEO pairs, the improvement is also promising for baselines longer than 1500 km. It should be noted that the percentages are still somewhat low at the group of 500–1000 km after correction, which might be due to the observation

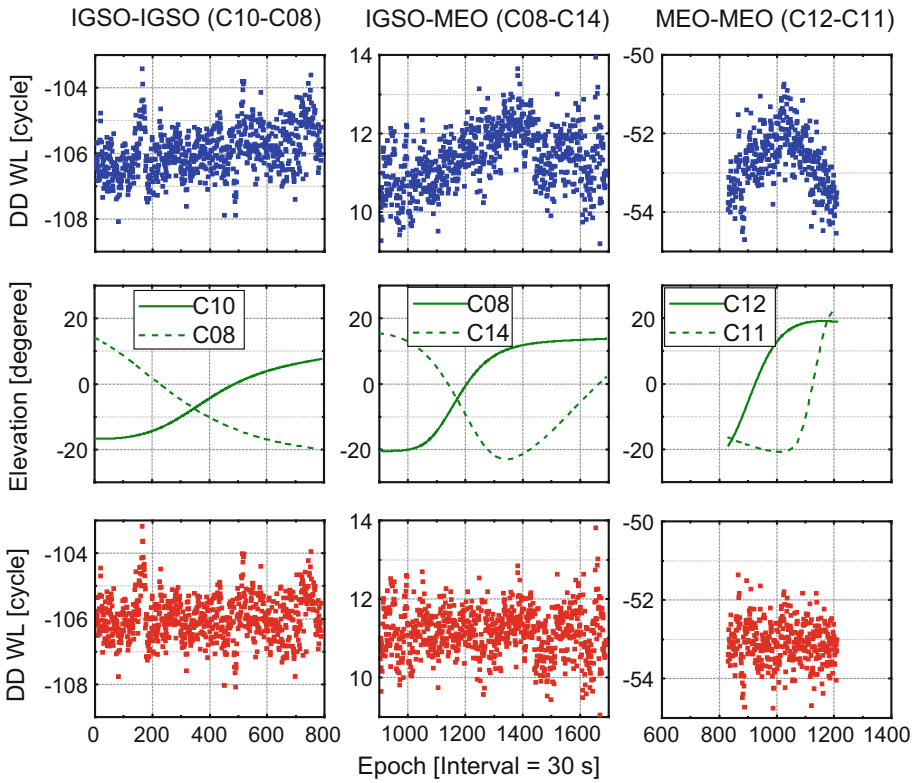

Fig. 2 BDS DD WL ambiguities without (*top row*) and with (*bottom row*) SCB correction, as well as the corresponding elevation differences of these two stations in respect to each satellite (*medium row*), over one exemplary baseline of about 2050 km, on DOY 040, 2015

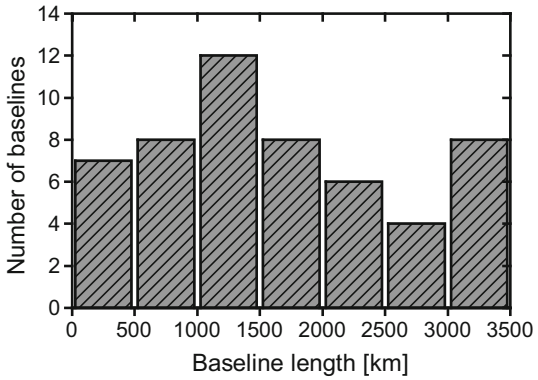

Fig. 3 Histogram showing the distribution of lengths of the independent baselines used in DD AR

time span, the data quality, or the imperfect SCB correction models.

POD results

Four different orbit solutions are calculated in this study: Solution 1 (float solutions without SCB correction), Solution 2 (float solutions with SCB correction), Solution 3 (AR solutions without SCB correction), and Solution 4 (AR solutions with SCB correction). We utilize orbit overlap comparison and SLR validation to assess and compare the quality of BDS IGSO and MEO orbits for these four solutions.

Orbit overlap comparison

As an internal validation of orbit accuracy, the orbit difference of the overlapped time span (24 h) between two different solutions is utilized. The last day of a 3-day orbital arc is compared with the first day of the 3-day arc that shifts two days backwards. Figure 6 illustrates the averaged RMS values of the overlapped orbit comparison in along-track, cross-track, and radial directions and 3D RMS for each IGSO and MEO satellite for the different solutions. The mean values of each satellite type for the different solutions are listed in Table 3. For these four solutions, the POD accuracies of MEO satellites are generally better than those of IGSO, and the RMS values of the radial direction are the smallest. Also, Solution 4, being AR solutions with SCB correction, shows the best internal consistency in all directions. The averaged 3D RMS is 10.46 and 6.89 cm, and the averaged RMS in radial direction reaches 3.25 and 1.96 cm for IGSO and MEO satellite, respectively.

For two float solutions, i.e., Solutions 1 and 2, the averaged RMS are almost the same. The 3D RMS values are 14.02 and 14.04 cm for IGSO, 10.97 and 10.03 cm for MEO satellite. This indicates that the BDS SCB has no significant impacts on float solutions for POD. For two AR solutions, the RMS values of Solution 3 are larger than those of Solution 4 for all satellites in all directions as shown in Fig. 6. The averaged 3D RMS is reduced from 12.10 to 10.46 cm for IGSO and from 8.22 to 6.89 cm for

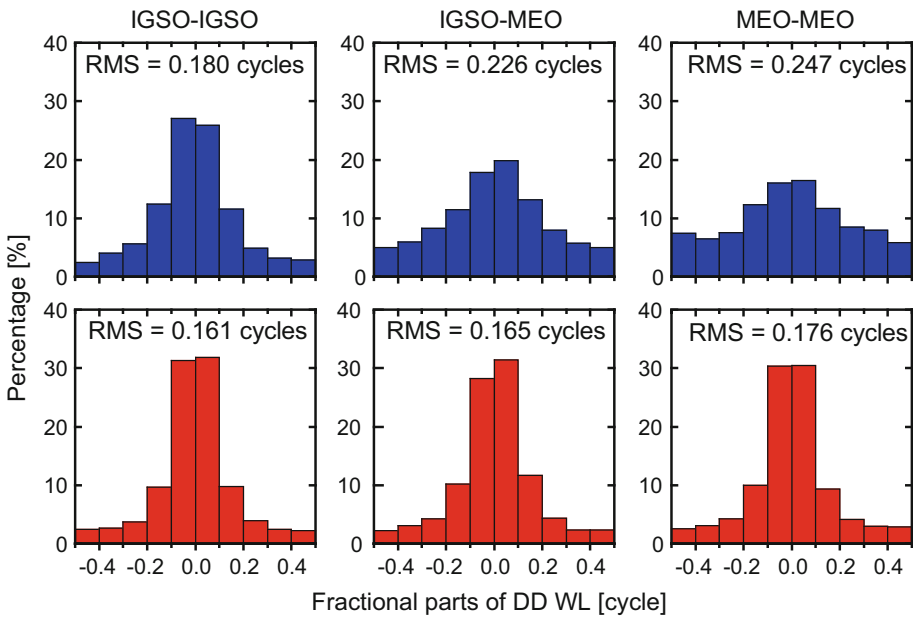

Fig. 4 Histogram indicating the distribution of fractional cycle parts of all DD WL ambiguities over all independent baselines for three satellite pairs, without (*top row*) and with (*bottom row*) SCB correction

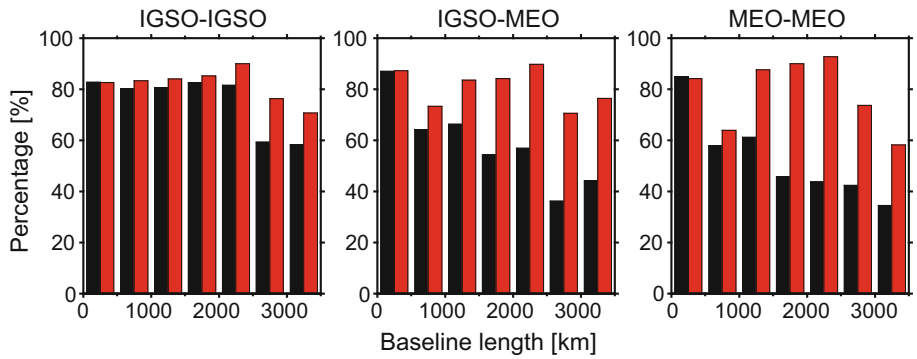

Fig. 5 Percentages of fractional parts of DD WL ambiguities within ± 0.2 cycles over baselines of various lengths as shown in Fig. 3, without (*black*) and with (*red*) SCB correction

MEO, which is the accuracy improvement of 13.6 and 16.2%. Such an improvement can be attributed to the correction of SCB, which improve the success rates of BDS WL AR as discussed in the previous section. It can be seen that AR of MEO satellites benefits from the SCB corrections more than IGSO.

Also, compared with Solution 1, the averaged RMS of Solution 3 shows a decrease of 19.4 and 9.4% for IGSO and 33.4 and 11.3% for MEO satellites in along- and cross-track directions, whereas an increase of 6.6 and 1.2% for IGSO and MEO in the radial direction. Compared with Solution 2, the averaged RMS of Solution 4 shows a decrease of 34.3 and 16.9% for IGSO and 38.9 and 17.8% for MEO satellites in along-track and cross-track directions. Moreover, the averaged RMS in radial direction is also reduced by 7.4% for IGSO and 19.7% for MEO satellites. These two comparisons not only further prove that the SCB cannot be neglected for BDS AR in POD, but also indicate that AR is an efficient method to improve BDS POD accuracy, especially for the along-track direction.

Regarding internal consistency, we conclude that BDS AR with SCB correction significantly improves the POD accuracy of IGSO and MEO satellites. The 3D mean RMSs are reduced from 14.02 to 10.46 cm for IGSO and from 10.97 to 6.89 cm for MEO satellites, with the improvement in overlap accuracy of 25.4 and 37.2%, respectively.

SLR validation

SLR observations provide an independent validation of estimated satellite orbits. The BDS satellites C01, C08, C10, and C11 equipped with laser retroreflector arrays are tracked by the International Laser Ranging Service (ILRS) network (Pearlman et al. 2002). Because the length of a POD arc is 3 days, only the orbital solutions of the middle day are used for validation. The SLR residuals, the differences between observed SLR values and the computed distance using the GNSS orbits and reference stations, are computed during the period of the experiment. Outliers exceeding 0.5 m are excluded and there are 176 normal

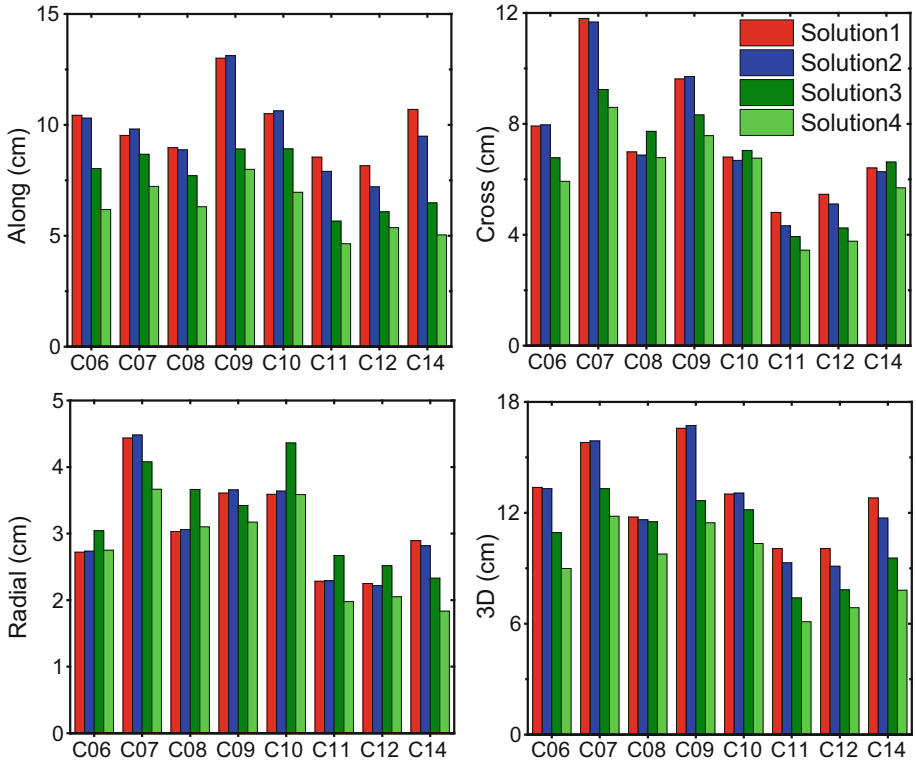

Fig. 6 Averaged RMS values of 1-day orbit overlap differences for individual IGSO and MEO satellite for four solutions. Note the different scales

Table 3 Mean RMS values of orbit overlap comparison of BDS IGSO and MEO for four different solutions (unit: cm)

Satellite type	Solutions	Along	Cross	Radial	3D
IGSO	Solution 1	10.49	8.63	3.48	14.02
	Solution 2	10.55	8.58	3.51	14.04
	Solution 3	8.45	7.82	3.71	12.10
	Solution 4	6.93	7.13	3.25	10.46
MEO	Solution 1	9.13	5.56	2.48	10.97
	Solution 2	8.20	5.23	2.44	10.03
	Solution 3	6.08	4.93	2.51	8.22
	Solution 4	5.01	4.30	1.96	6.89

points (NP) available for C08, 93 NPs for C10, and 163 NPs for C11 after removal of outliers. The offsets, standard deviation and RMS values of SLR residuals for four solutions are listed in Table 4.

We can see clearly that AR solutions with SCB correction show the best accuracy among the four solutions. After AR the offsets are significantly reduced, especially for C10 satellite, from −5 to about 0.3 cm. Compared with Solution 1, the RMS values of Solution 4 are reduced from 7.68 to 6.69 cm for IGSO and from 3.28 to 3.08 cm for MEO satellites, with the reduction percentage of 12.9 and 6.1%, respectively. Although the amplitude of the RMS reduction compared with float solutions is not as significant as that in the overlap comparison, it confirms the improvement in the BDS orbit quality through AR with SCB correction.

Conclusions

Different from other GNSS systems, BDS code measurements are affected by the SCB, preventing successful BDS AR of long baselines which widely exist in the ground

Table 4 SLR residuals for BDS C08, C10 and C11 orbital solutions (unit cm)

Solutions	C08 (IGSO)			C10 (IGSO)			C11 (MEO)		
	Offset	STD	RMS	Offset	STD	RMS	Offset	STD	RMS
Solution 1	−0.51	7.14	7.16	−5.15	6.39	8.20	−0.18	3.27	3.28
Solution 2	−0.55	7.12	7.15	−5.12	6.41	8.20	−0.19	3.43	3.43
Solution 3	0.49	7.71	7.73	−0.26	6.13	6.13	0.10	3.11	3.11
Solution 4	0.20	7.76	7.76	0.36	5.61	5.62	0.17	3.08	3.08

tracking network used in POD. We have investigated the impacts of the SCB on BDS DD AR, according to different types of satellites and different lengths of baselines by theoretical and numerical analysis. Due to the dependence of the SCB on elevation angle, the lower orbit satellites, i.e., MEO satellites, and longer baselines were largely affected by SCB on WL AR.

Based on the impact of SCB on BDS AR and the contribution of AR toward improving POD, we have carried out BDS POD using one month of observations from 58 stations of the MGEX and Fugro network in four cases. The orbit solutions obtained from these four cases, i.e., float solutions, float solutions with SCB correction, AR solutions, and AR solutions with SCB correction, are compared by analyzing orbit overlap differences and SLR residuals. The comparison of float solutions with and without SCB correction suggests that the SCB has no significant impacts on float solutions, and the comparison of AR solutions with and without SCB correction suggests that SCB is not negligible for BDS AR in POD. Furthermore, the results of AR solutions with SCB correction show the best orbit accuracy regarding internal consistency and SLR validation. The mean RMS of orbit overlap differences in the radial direction reach to 3.25 and 1.96 cm for IGSO and MEO satellite, respectively. The 3D overlapping accuracy improves by 25.4% for IGSO and 37.2% for MEO, which shows a significant contribution as for GPS, especially for MEO.

The presented method of AR with SCB correction can be applied to the MGEX ACs data processing of BDS POD to improve IGSO and MEO satellites orbital products. It is worthwhile to mention that the orbital accuracy of BDS GEO satellites is still very poor. The problem that exists in GEO AR, especially for long baseline, needs to be solved. Therefore, further studies will focus on improvement in GEO AR performance and GEO orbit accuracy.

Acknowledgements The authors are very grateful to IGS MGEX campaign and Fugro for providing BDS tracking data. This work is supported by the National Nature Science Foundation of China (Nos. 41404032, 41674004, 41574030), Natural Science Foundation of Hubei Province (No. 2014CFB168), and Fundamental Research Funds for the Central Universities (No. 2042016kf0185).

References

Blewitt G (1989) Carrier phase ambiguity resolution for the Global Positioning System applied to geodetic baselines up to 2000 km. J Geophys Res 94(B8):10187–10203. doi:10.1029/JB094iB08p10187

CSNO (2013) BeiDou navigation satellite system signal in space interface control document, Open Service Signal (Version 2.0). China Satellite Navigation Office (CSNO)

Dai X, Ge M, Lou Y, Shi C, Wickert J, Schuh H (2015) Estimating the yaw-attitude of BDS IGSO and MEO satellites. J Geod 89(10):1005–1018. doi:10.1007/s00190-015-0829-x

Dong D, Bock Y (1989) Global positioning system network analysis with phase ambiguity resolution applied to crustal deformation studies in California. J Geophys Res 94(B4):3949–3966. doi:10.1029/JB094iB04p03949

Dow JM, Neilan RE, Rizos C (2009) The International GNSS Service in a changing landscape of global navigation satellite systems. J Geod 83(3–4):191–198. doi:10.1007/s00190-008-0300-3

Gao W, Gao C, Pan S, Wang D, Deng J (2015) Improving ambiguity resolution for medium baselines using combined GPS and BDS dual/triple-frequency observations. Sensors 15(11):27525–27542. doi:10.3390/s151127525

Ge M, Gendt G, Dick G, Zhang FP (2005) Improving carrier-phase ambiguity resolution in global GPS network solutions. J Geod 79(1–3):103–110. doi:10.1007/s00190-005-0447-0

Ge M, Zhang H, Jia X, Song S, Wickert J (2012) what is achievable with the current compass constellation? ION GNSS 2012, Institute of Navigation, Nashville, Tennessee, USA, September 17–21, pp 331–339

Gisbert JVP, Batzilis N, Risueño GL, Rubio JA (2012) GNSS payload and signal characterization using a 3 m dish antenna. ION GNSS 2012, Institute of Navigation, Nashville, Tennessee, USA, September 17–21, pp 347–356

Guo J, Xu X, Zhao Q, Liu J (2015) Precise orbit determination for quad-constellation satellites at Wuhan University: strategy, result validation, and comparison. J Geod 90(2):143–159. doi:10.1007/s00190-015-0862-9

Guo F, Li X, Zhang X, Wang J (2016a) Assessment of precise orbit and clock products for Galileo, BeiDou, and QZSS from IGS multi-GNSS experiment (MGEX). GPS Solut. doi:10.1007/s10291-016-0523-3

Guo J, Chen G, Zhao Q, Liu J, Liu X (2016b) Comparison of solar radiation pressure models for BDS IGSO and MEO satellites with emphasis on improving orbit quality. GPS Solut. doi:10.1007/s10291-016-0540-2

Hatch R (1982) The synergism of GPS code and carrier measurements. In: Proceedings of the third international symposium on satellite doppler positioning at Physical Sciences Laboratory of New Mexico State University, Feb. 8–12, vol 2, pp 1213–1231

Hauschild A, Montenbruck O, Sleewaegen J-M, Huisman L, Teunissen PJG (2012) Characterization of compass M-1 signals. GPS Solut 16(1):117–126. doi:10.1007/s10291-011-0210-3

He L, Ge M, Wang J, Wickert J, Schuh H (2013) Experimental study on the precise orbit determination of the BeiDou navigation satellite system. Sensors 13(3):2911–2928. doi:10.3390/s130302911

Kouba J, Héroux P (2001) Precise point positioning using IGS orbit and clock products. GPS Solut 5(2):12–28. doi:10.1007/pl00012883

Li X, Ge M, Dai X, Ren X, Fritsche M, Wickert J, Schuh H (2015) Accuracy and reliability of multi-GNSS real-time precise positioning: GPS, GLONASS, BeiDou, and Galileo. J Geod 89(6):607–635. doi:10.1007/s00190-015-0802-8

Liu J, Ge M (2003) PANDA software and its preliminary result of positioning and orbit determination. Wuhan Univ J Nat Sci 8(2B):603–609. doi:10.1007/BF02899825

Liu Y, Ye S, Song W, Lou Y, Chen D (2016) Integrating GPS and BDS to shorten the initialization time for ambiguity-fixed PPP. GPS Solut. doi:10.1007/s10291-016-0525-1

Lou Y, Liu Y, Shi C, Yao X, Zheng F (2014) Precise orbit determination of BeiDou constellation based on BETS and MGEX network. Scientific Rep 4:4692. doi:10.1038/srep04692

Lou Y, Gong X, Gu S, Zheng F, Feng Y (2016) Assessment of code bias variations of BDS triple-frequency signals and their impacts on ambiguity resolution for long baselines. GPS Solut. doi:10.1007/s10291-016-0514-4

McCarthy DD, Petit G (2003) IERS conventions 2003. IERS technical note No. 32. Bundesamt fuer Kartographie und Geodaesie, Frankfurt am Main

Melbourne WG (1985) The case for ranging in GPS-based geodetic systems. In: Proceedings of the first international symposium on precise positioning with the global positioning system, Rockville, 15–19 April, pp 373–386

Montenbruck O, Hauschild A, Steigenberger P, Hugentobler U, Teunissen P, Nakamura S (2012) Initial assessment of the COMPASS/BeiDou-2 regional navigation satellite system. GPS Solut 17(2):211–222. doi:10.1007/s10291-012-0272-x

Montenbruck O, Chris R, Robert W, Georg W, Ruth N, Urs H (2013) Getting a grip on multi-GNSS The international GNSS service MGEX campaign. GPS World 24(7):44–49

Montenbruck O, Steigenberger P, Khachikyan R, Weber G, Langley RB, Mervart L, Hugentobler U (2014) IGS-MGEX: preparing the ground for multi-constellation GNSS science. Inside GNSS 9(1):42–49

Pearlman MR, Degnar JJ, Bosworth JM (2002) The international laser ranging service. Adv Space Res 30:135–143. doi:10.1016/S0273-1177(02)00277-6

Qu L et al (2015) BDS/GNSS real-time kinematic precise point positioning with un-differenced ambiguity resolution. In: Sun JJW, Wu H, Lu M (eds) Proceedings of China satellite navigation conference (CSNC) 2015, Springer, Berlin, pp 13–29. doi:10.1007/978-3-662-46632-2_2

Shi C, Zhao Q, Geng J, Lou Y, Ge M, Liu J (2008) Recent development of PANDA software in GNSS data processing. In: Proceedings of SPIE 7285, international conference on earth observation data processing and analysis (ICEODPA). doi:10.1117/12.816261

Shi C et al (2012) Precise orbit determination of Beidou satellites with precise positioning. Sci China Earth Sci 55(7):1079–1086. doi:10.1007/s11430-012-4446-8

Shi C, Zhao Q, Hu Z, Liu J (2013) Precise relative positioning using real tracking data from COMPASS GEO and IGSO satellites. GPS Solut 17(1):103–119. doi:10.1007/s10291-012-0264-x

Springer T, Beutler G, Rothacher M (1999) A new solar radiation pressure model for GPS satellites. GPS Solut 2(3):50–62

Steigenberger P, Hugentobler U, Hauschild A, Montenbruck O (2013) Orbit and clock analysis of compass GEO and IGSO satellites. J Geod 87(6):515–525. doi:10.1007/s00190-013-0625-4

Tegedor J, Øvstedal O, Vigen E (2014) Precise orbit determination and point positioning using GPS, GLONASS, Galileo and BeiDou. J Geod Sci 4(1):65–73. doi:10.2478/jogs-2014-0008

Wanninger L, Beer S (2015) BeiDou satellite-induced code pseudo-range variations: diagnosis and therapy. GPS Solut 19(4):639–648. doi:10.1007/s10291-014-0423-3

Wübbena G (1985) Software developments for geodetic positioning with GPS using TI-4100 code and carrier measurements. In: Proceedings of the first international symposium on precise positioning with the global positioning system, Rockville, 15–19 April, pp 403–412

Zhang X, He X (2015) Performance analysis of triple-frequency ambiguity resolution with BeiDou observations. GPS Solut 20(2):269–281. doi:10.1007/s10291-014-0434-0

Zhang R, Zhang Q, Huang G, Wang L, Qu W (2015) Impact of tracking station distribution structure on BeiDou satellite orbit determination. Adv Space Res 56(10):2177–2187. doi:10.1016/j.asr.2015.07.045

Zhao Q, Guo J, Li M, Qu L, Hu Z, Shi C, Liu J (2013) Initial results of precise orbit and clock determination for COMPASS navigation satellite system. J Geod 87(5):475–486. doi:10.1007/s00190-013-0622-7

Zhao Q, Dai Z, Hu Z, Sun B, Shi C, Liu J (2015) Three-carrier ambiguity resolution using the modified TCAR method. GPS Solut 19(4):589–599. doi:10.1007/s10291-014-0421-5

Tao Geng is an associate professor at GNSS Research Center, Wuhan University, China. He received his Ph.D. in Geodesy and Surveying Engineering from Wuhan University in 2009. From February 2013 to February 2014, he was a visiting scholar at Ohio State University. His research interest focuses on precise GNSS orbit determination and positioning.

Xin Xie is currently a Ph.D. candidate at GNSS Research Center, Wuhan University. He received his B.Sc. degree in 2014 from China University of Geosciences. His current research mainly focuses on precise orbit determination of GNSS and high-precision positioning using GNSS.

Qile Zhao is a professor of GNSS Research Center of Wuhan University. He received his PhD degree in Wuhan University in 2004. In 2006–2007, as a postdoctoral fellow, he did his postdoctoral program in DEOS, Delft University of Technology, the Netherlands. His current research interests are precise orbit determination of GNSS and low earth orbit satellites, and high-precision positioning using GPS, Galileo and BDS system.

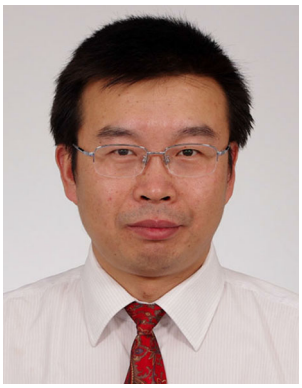

Xianglin Liu is a senior geodesist and the lead of GNSS R&D group at Fugro Intersite B.V., the Netherlands. He received his Ph.D. degrees at Delft University of Technology and Wuhan University. His main research focuses on PPPRTK with multi-GNSS and multifrequency observations.

Jingnan Liu graduated from the former Wuhan College of Surveying and Mapping in 1967 and received his master's degree in 1982. He was elected Academician of the Chinese Academy of Engineering in 1999. He has been a member of the Science and Technology Committee, Ministry of Education of China, in 1997–2009 and as an editorial board member of GPS Solutions in 1998–2000. He is currently an executive member of the council, Chinese Society for Geodesy Photogrammetry and Cartography; the editorial board member of GPS World; and the coordinator of International GPS Geodynamics Services. His current research interests are satellite precise orbit determination.